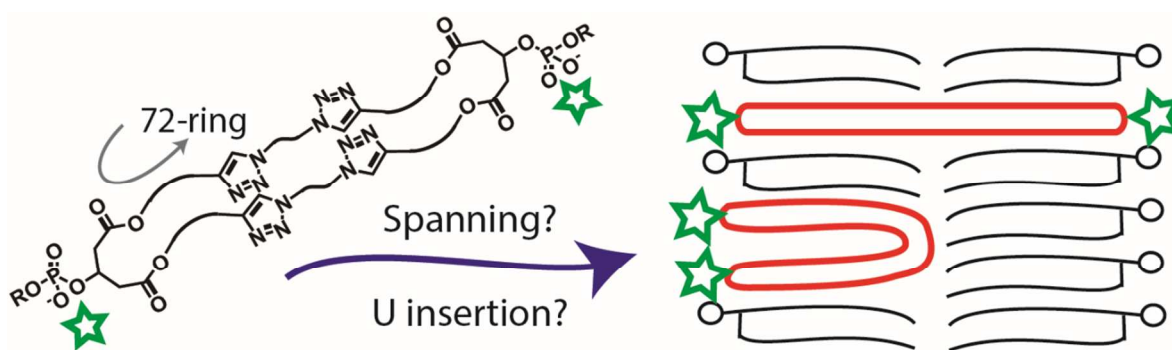


# A membrane-spanning macrocyclic bolaamphiphile lipid mimic of archaeal lipids

Gavin M. Mitchell, Amelia Hesketh, Christie Lombardi, Cally Ho, and Thomas M. Fyles\*

Department of Chemistry, University of Victoria, Box 1700 STN CSC, Victoria BC V8W 3V6

Whilst this paper discloses no aromatic novelty, it nonetheless  
honours Reg Mitchell's collegial mentoring over many decades.



Author for correspondence:

T.M. Fyles

[tmf@uvic.ca](mailto:tmf@uvic.ca)

Tel: 250 721 7192

Fax: 250 721 7147

**21 Abstract**

22 The synthesis of a 72-membered macrocyclic tetraester bolaamphiphile is accomplished in six  
23 chemical steps from commercially available starting materials using copper-accelerated azide-  
24 alkyne coupling to close the macrocycle in high yield. Related diester amphiphiles and an  
25 acyclic tetraester bolaamphiphile were also prepared. The set of lipids bearing nitrophenyl  
26 phosphate head groups were incorporated into phospholipid vesicles but failed to undergo  
27 phosphate hydrolysis in basic conditions, undergoing efficient elimination in competition. The  
28 same lipid cores bearing phosphate-linked nitrobenzoxadiazole (NBD) head groups also  
29 incorporated into phospholipid vesicles and the NBD fluorescence was quenched with cobalt  
30 ions. The proportion of membrane-spanning bolaamphiphiles was determined from the ratio of  
31 cobalt quenching in the presence and in the absence of a detergent. The macrocyclic  
32 bolaamphiphile is incorporated into phospholipid vesicles such that  $48 \pm 4\%$  of the NBD head  
33 groups are in the outer leaflet, consistent with a membrane-spanning orientation. The acyclic  
34 bolaamphiphile is incorporated with  $75 \pm 3\%$  of the NBD head groups accessible to quencher in  
35 the absence of a detergent suggesting U-shaped incorporation in the outer leaflet of the bilayer  
36 membrane. In ring size and spanning ability, the macrocyclic bolaamphiphile mimics naturally  
37 occurring macrocyclic archaeal lipids.

38

**39 Keywords:**

40 macrocyclic lipid, membrane-spanning, bolaamphiphile, synthesis, fluorescence, quenching

41

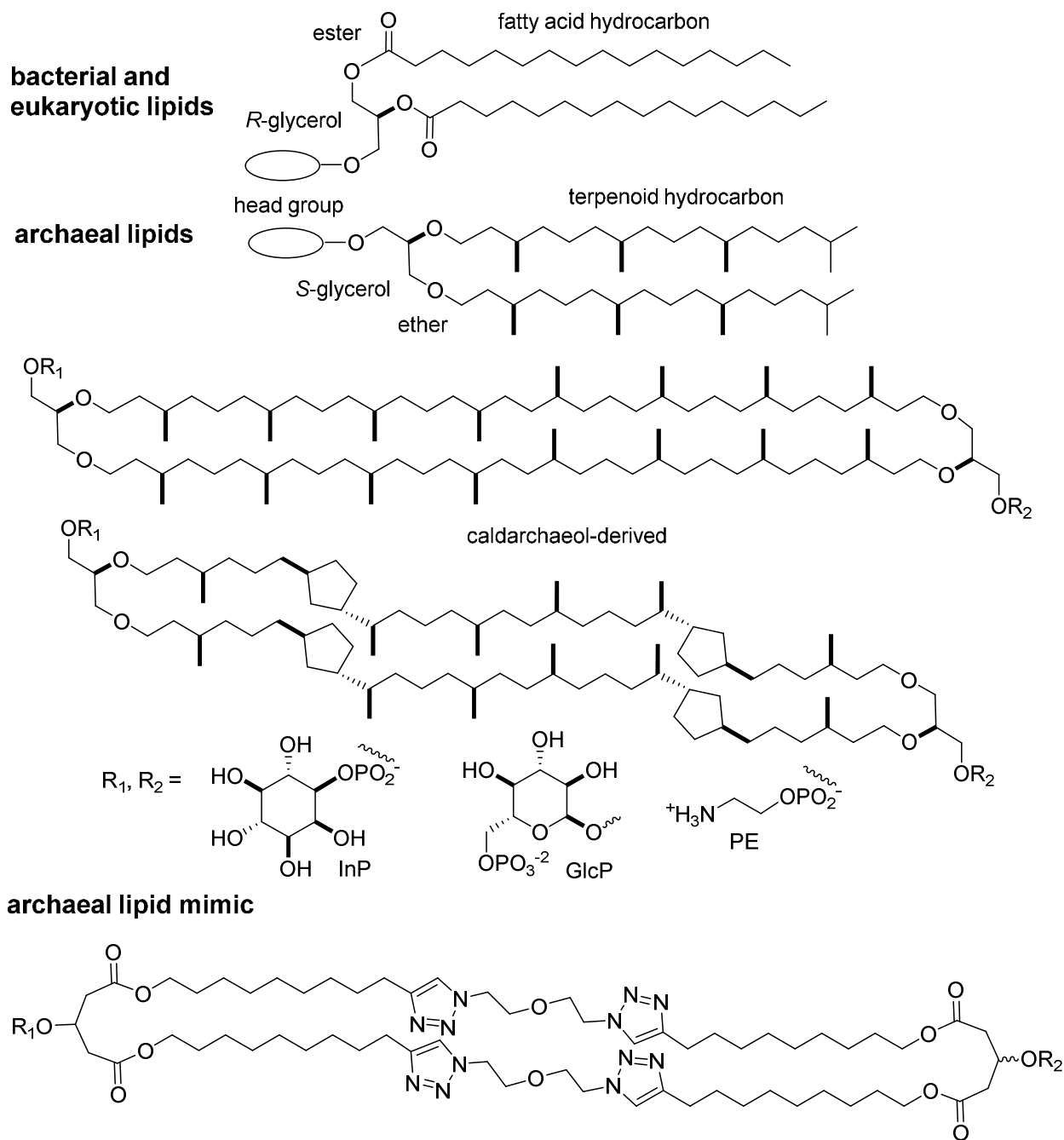
42 **Plain language summary**

43 How can some bacteria survive in hot, acidic, or very salty water? One idea is that the lipids in the cell  
44 membranes provide the chemical and mechanical stability to hold the cell together. The lipids extracted  
45 from these bacteria support this idea – they contain unreactive groups and they are long enough to reach  
46 across a cell membrane so could hold the two sides of the membrane together like a reinforcing rod. But  
47 natural compounds are hard to isolate and purify, and they cannot easily be made so it is hard to prove  
48 that the compounds do what we imagine might they do. To test this idea in a simple way, and to make  
49 pure compounds that might be useful in drug-delivery applications, we need to design compounds that  
50 mimic the natural lipids. This study shows how to make one possible mimic efficiently in a few chemical  
51 steps together with some simpler analogs. We also show that the designed mimic does in fact span a  
52 typical membrane using a new method to determine how the compound is located in the membrane. We  
53 are still not sure if this type of spanning molecule does reinforce the membrane – but we do have a tool to  
54 test that question directly.

55

## 56 Introduction:

57 The lipids of species of the domain *Archaea* are distinct from those of eukaryotes and  
58 bacteria<sup>1,2</sup>. While the lipids of the latter two domains are largely fatty-acid derived esters of *R*-  
59 1,2-glycerol-phosphoesters, archaeal lipids are terpene-derived ethers of *S*-1,2-glycerol with the  
60 3-position bearing either a phospho- or a glyco-linked headgroup (Fig. 1). Whatever their role in  
61 early evolution<sup>3</sup>, modern *Archaea* species occupy harsh environments; extreme halophiles live in  
62 warm high-salt brines, thermoacidophiles require hot acidic environments, and extreme  
63 thermophiles grow optimally at temperatures above 80 °C<sup>1,2</sup>. The common assumption is that  
64 the chemical composition of the lipid membranes of *Archaea* facilitates survival in extreme  
65 conditions through the additional chemical stability of hydrolysis-resistant ether linkages in the  
66 lipid core (Figure 1). Additionally, archealipids contain apparent tail-to-tail dimer lipids based  
67 on a macrocyclic *caldarchaeol* lipid core. The hydrocarbon segments of the caldarchaeols can  
68 be diphytane- $\alpha,\omega$ -diols, or are additionally oxidized to incorporate up to eight *trans*-1,3-  
69 cyclopentano-units<sup>1,2</sup>. Caldarcheol-derived lipids are *bolaamphiphiles* bearing two polar head  
70 groups bridged by a significant non-polar region<sup>4</sup>. As such they are potentially capable of  
71 spanning a bilayer composed of single headed archaeal lipids and there is evidence that  
72 membrane-spanning occurs<sup>5</sup>. Another common assumption is that the membrane-spanning  
73 components impart additional mechanical stability to the bilayer membranes of *Archaea*<sup>1,2</sup>.



74

75 *Figure 1.* The lipid structures of *Archaea* differ from those of eukaryotes in the presence of the  
 76 opposite glycerol-stereochemistry, ether linkages, saturated terpenoid hydrocarbon tails, and  
 77 macrocyclic lipid cores. The proposed archaeal lipid mimic is a hybrid based on a macrocyclic  
 78 tetraester.

79

80

81 The combination of properties presented by archaeal lipids leads to potential biotechnology  
82 applications<sup>2,6</sup>. Liposomes from natural archaeal lipids, known as *archaeosomes*, are more  
83 physically stable than conventional liposomes based on ester-linked phospholipids<sup>7,8</sup>. In  
84 particular, archaeosomes are thermally resistant and can maintain entrapment integrity even  
85 when autoclaved<sup>9</sup>. Archaeosomes are also more susceptible to uptake by phagocytic cells than  
86 liposomes of ester phospholipids<sup>10</sup> leading to their utility as adjuvants in the development of  
87 antibodies<sup>2,11,12</sup>. The wider use of archaeosomes is directly limited by availability of archaeal  
88 lipids derived as mixtures from natural sources<sup>7</sup>. The remarkable total synthesis of the 72-  
89 membered macrocyclic tetraether archaeal lipid core<sup>13</sup> is lengthy and does not readily lead itself  
90 to scale-up or to the preparation of lipids with head group dissymmetry as commonly found in  
91 naturally-derived samples<sup>2,6,7</sup>.

92  
93 Synthetic bolaamphiphiles proposed as archaeal lipid mimics have been explored for over three  
94 decades<sup>4,14,15</sup>. Synthetic mimics can offer pure samples of defined structures, but essential  
95 structural simplifications to facilitate synthesis also loosen the bounds of mimicry and may result  
96 in substantially different functions. Early work focussed on macrocyclic bolaamphiphiles  
97 bearing short (C<sub>12</sub>-C<sub>18</sub>) spans that produced much thinner monolayer membranes where it is clear  
98 that the macrocycles must be membrane-spanning<sup>16</sup>. An alternative approach involves  
99 bolaamphiphiles with a single long hydrophobic strand (ca 3 nm) separating two head-  
100 groups<sup>14,17,18</sup>. It is not clear in these cases that the bolaamphiphile is membrane-spanning when  
101 mixed with bilayer-forming phospholipids, and U-shaped insertion is common<sup>18,19</sup>. U-shaped  
102 insertions of linear strands are associated with enhanced membrane permeability<sup>19,20</sup> but  
103 spanning insertions are uncorrelated with permeability enhancement; some do, others do not<sup>18,21</sup>.

104 Naturally-derived archaeal lipids do not necessarily adopt spanning conformations and may also  
105 adopt U-shaped organization in films and vesicles<sup>7,22</sup> which may also influence the water and  
106 ionic permeability of archaeosomal membranes<sup>23</sup>. The fine balance between spanning and U-  
107 shape in bolaamphiphiles based on a single long strand appears to be related to lipid-packing  
108 considerations, albeit in single-component films and aggregates<sup>15,17,24,25</sup>.

109  
110 From a biotechnology perspective, applications based on pure single-component archaeal lipid  
111 mimics are unlikely; mixtures with additional lipid components will be required to control  
112 particle size, charge, storage stability, and off-target effects including toxicity<sup>26,27</sup>. In such a  
113 lipid-based delivery system, the archaeal lipid mimic would be a minor component designed to  
114 provide mechanical stabilization of bilayers predominantly composed of ester-linked  
115 phospholipids. It is therefore critical to initially establish that candidate archaeal lipid mimics  
116 are miscible in phospholipid bilayers and adopt a membrane-spanning orientation without  
117 enhancing membrane permeability. Thereafter it will be possible to establish if the mimic does  
118 impart the expected mechanical stabilization of the lipid mixture formulated for the particular  
119 application and thus result in any subsequent benefits related to the archaeal lipid mimic.

120  
121 Our potentially membrane-spanning macrocyclic archaeal lipid mimic is given in Figure 1. The  
122 design is driven by a combination of practical considerations and experience derived from linear  
123 oligoester ion channels<sup>19,20,28-31</sup>. Good phospholipid miscibility is associated with extended alkyl  
124 esters<sup>32,33</sup> and the use of glutarate diesters in place of glycerol diesters is both a reliable and  
125 simplifying synthetic strategy<sup>28,34</sup>. The 1,2,3-triazole produced via copper-catalyzed alkyne-  
126 azide coupling (CuAAC)<sup>35</sup> also has good lipid miscibility in conjunction with esters elsewhere in

127 the structure<sup>33</sup> and has previously featured in single-chain archaeal lipid mimics designed to  
128 enhance membrane permeability via flip-flop which necessarily requires a U-shaped insertion  
129 <sup>36,37</sup>. Membrane-inactive *per*-substituted cyclodextrins bearing triazoles and esters<sup>38</sup> suggest that  
130 there is no inherent membrane destabilizing character to triazoles or esters provided U-shaped  
131 insertions can be avoided. The high reaction rate and efficiency and the potential for Cu-centered  
132 templation in CuAAC has been widely exploited in macrocyclizations<sup>39-41</sup>. The target  
133 macrocycle is potentially derived from a commercially available bis-azide and 10-undecyn-1-ol,  
134 the longest commercially available  $\omega$ -hydroxy alkyne, which coincidentally gives an estimated  
135 extended hydrophobic strand length of 3.5 nm – well suited to the requirements of a  
136 phospholipid bilayer. Also coincidentally, the mimic contains a 72-membered ring as in the  
137 caldarchaeols.

138  
139 The goal of this study is to explore the synthesis of the potentially membrane-spanning  
140 macrocycle proposed in Figure 1, and to establish if it is both miscible and membrane-spanning  
141 in a phospholipid bilayer vesicle. Related compounds are also prepared to assist with the  
142 development of the synthesis and of the assay for membrane-spanning proportion.

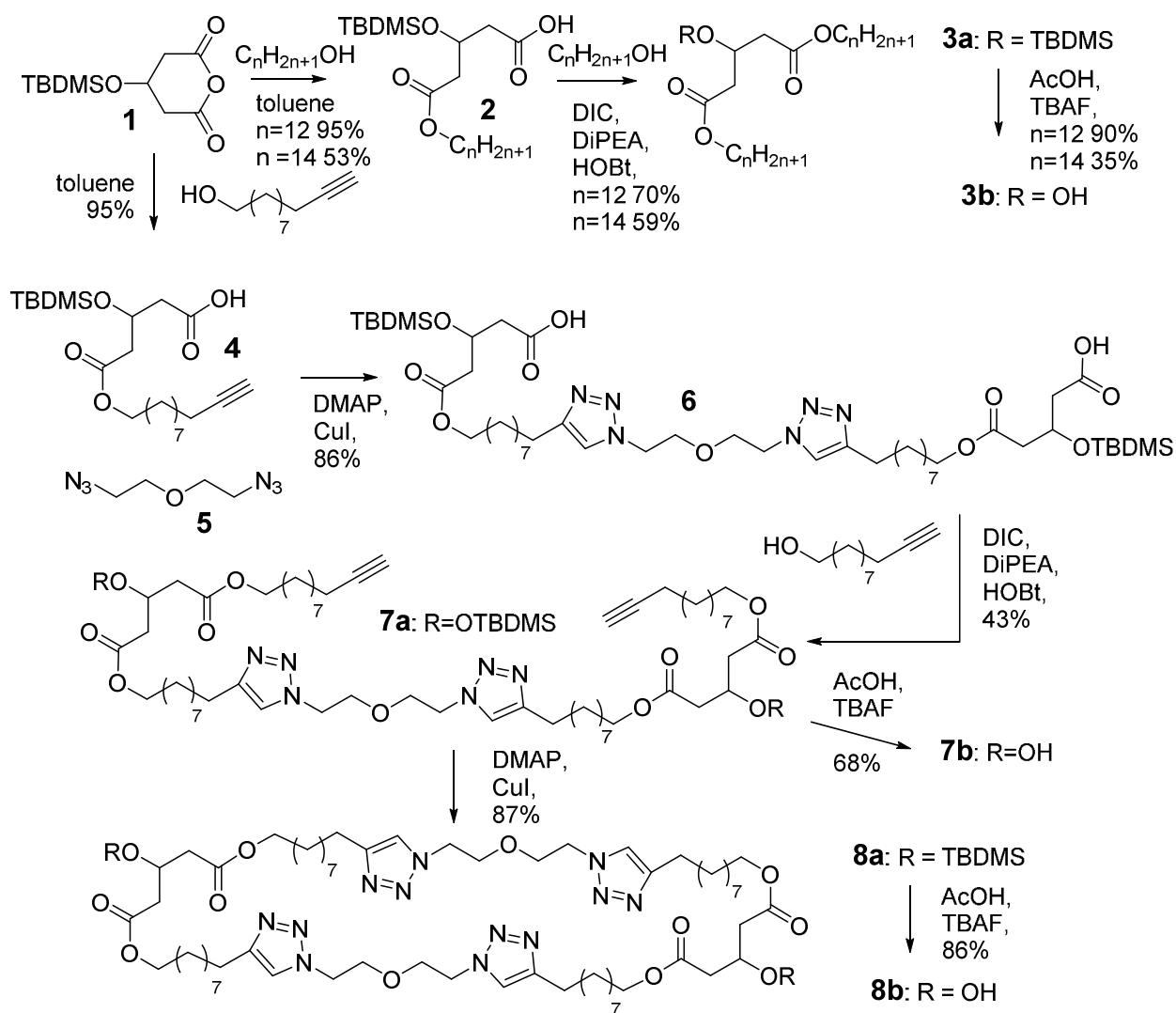
## 144 **Results and Discussion**

### 145 *Synthesis*

146 The synthesis of macrocyclic diol **8b** and related compounds is given in Scheme 1. The  
147 protected 3-hydroxyglutarate monoester of 10-undecyn-1-ol was readily prepared using a small  
148 excess of the anhydride **1** to drive the process. Compound **4** is unstable in solutions containing  
149 any protic solvent, reverting to starting materials, so chromatographic purification was not

150 possible. A procedure involving removal of excess **1** by low temperature crystallization proved  
 151 effective. Purifications of previous glutarate monoesters of this type also relied on differential  
 152 solubility, but of the product monoester not the anhydride<sup>28,31</sup>. The same procedure produced  
 153 compound **2** from 1-dodecanol (n = 12) or 1-tetradecanol (n = 14) albeit in lower yields due to  
 154 different product solubility under the low-temperature crystallization conditions.

155



156

157 *Scheme 1: Synthetic routes to the lipid cores of acyclic and macrocyclic esters.*

158

159 The first of the projected CuAAC reactions of alkyne **4** with bis-azide **5** required extensive  
160 optimization of solvent, base, copper source, time, and temperature<sup>42</sup>. A key variable appeared  
161 to be the base – dimethylaminopyridine in the optimized protocol – as other bases lead to  
162 incomplete reaction, ester cleavage, or deprotection to various degrees. Close control of the 2:1  
163 stoichiometry allowed isolation of the product **6** solely by extractive workup. Compound **6** is a  
164 very sticky material that readily entraps solvent which must be removed at high vacuum. Diacid  
165 **6** was then converted to the tetraester **7a** using a previously developed esterification protocol<sup>29</sup>  
166 for similar glutarate diesters. The same protocol produced **3a** from **2** in variable yields related to  
167 purification losses.

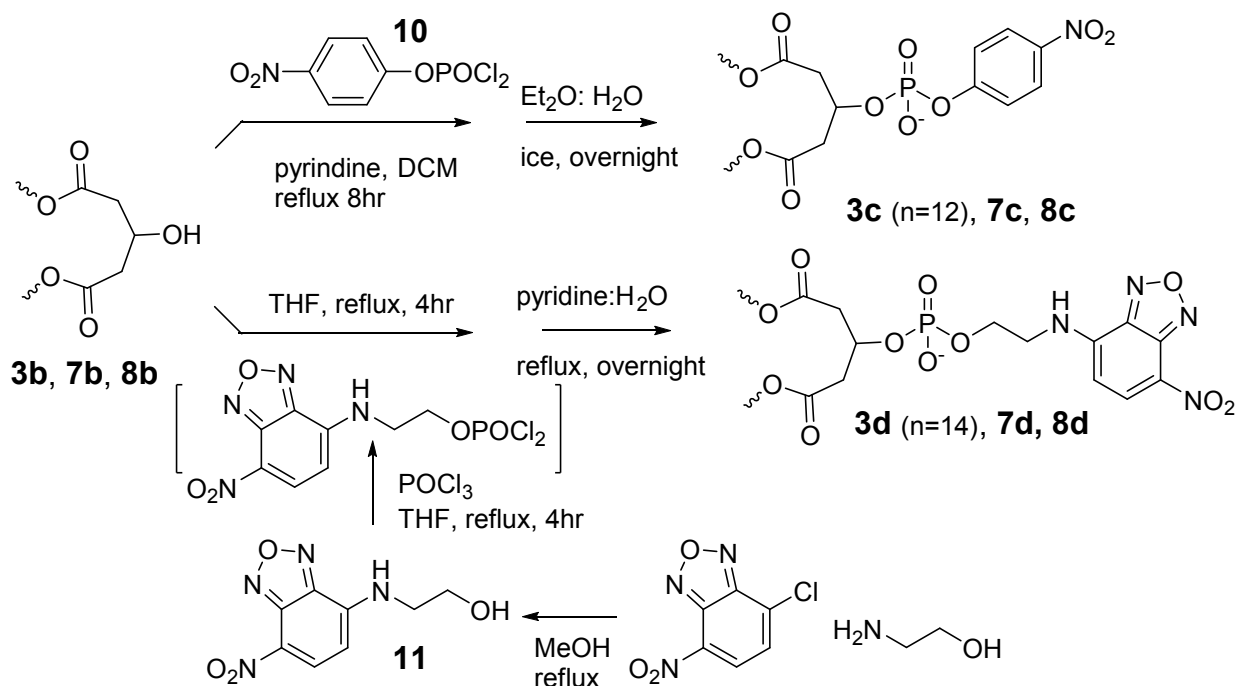
168  
169 Finally the diyne **7a** was subjected to the optimized CuAAC conditions with **5** to produce  
170 macrocycle **8a** in a remarkable yield of 87%. A key parameter in this reaction was the final  
171 concentration (0.11 M product); at higher concentrations some product appeared to be formed  
172 but occurred in a poorly soluble and intractable gel<sup>43</sup> containing Cu(II) as judged from a pale  
173 blue color in air-exposed samples, while at a low concentration the product did not form fast  
174 enough to compete with side-reactions. Samples contaminated with Cu(II) gave poor NMR  
175 spectra with multiple triazole signals in both <sup>1</sup>H and <sup>13</sup>C-nmr spectra suggesting that a  
176 component of the good macrocyclization yield was related to Cu templating. Extensive  
177 extraction with EDTA during workup was required to produce clean samples of **8a**, freely  
178 soluble in chloroform, with the expected NMR spectra and mass spectrum identified as that of a  
179 sodium adduct molecular ion.

180

181 Deprotection using TBAF-acetic acid afforded the diol **8b** in apparently quantitative yield with  
182 losses related to purification only. The same protocol produced **3b** from **3a** and **7b** from **7a**.  
183 Analysis of incomplete reaction mixtures by ESI-MS provided further evidence that the product  
184 from **8a** was the expected macrocycle as only three species were detected corresponding to the  
185 Na<sup>+</sup> adducts of **8a** (1459.95 m/z), **8b** (1231.80 m/z), and the intermediate mono TBDMS species  
186 (1346.86 m/z). Had the starting **8a** contained a proportion of oligomers hidden in the  
187 complexities of the NMR spectra, these would have produced additional intermediate partially  
188 cleaved structures that would have shown additional ESI-MS signals. Compound **8b** is available  
189 in 26% yield over five steps from the starting anhydride **1**.

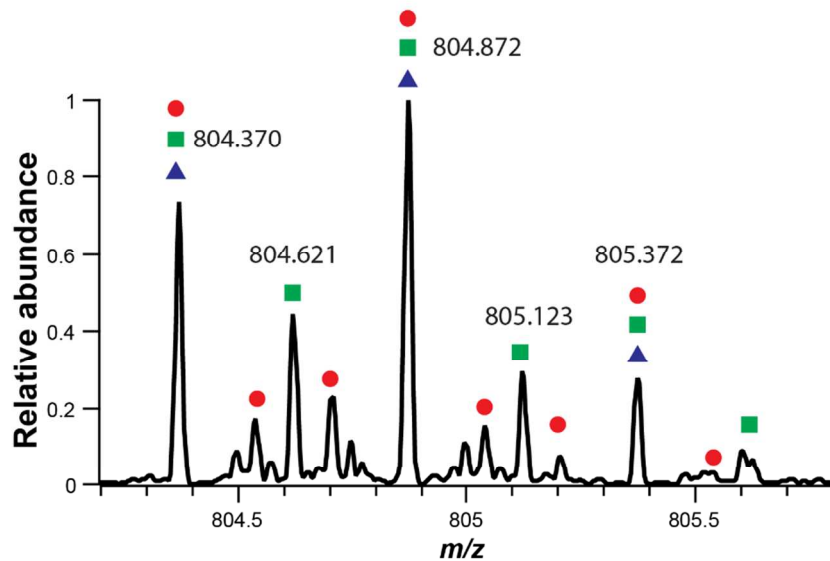
190  
191 Conversion of the core lipids **8b**, **7b**, and **3b** to amphiphiles requires that polar head groups be  
192 appended. A reported assay for membrane-spanning proportion (discussed below) uses a  
193 nitrophenyl phosphate head group, so the first series of compounds was prepared using 4-  
194 nitrophenyl phosphorodichloridate (**10**) to form the phosphate diesters **3c** (n = 12), **7c**, and **8c**  
195 after pyridine-water hydrolysis (Scheme 2)<sup>44</sup>. The amphiphiles are poorly soluble in pure solvents  
196 but adequately soluble in 5% methanol in dichloromethane. Chromatographic losses are very  
197 significant so the products were isolated and purified by a dissolution-precipitation sequence to  
198 remove excess reagents. The NMR spectra of these products are broadened but the integrations in  
199 the <sup>1</sup>H- NMR spectra are consistent with the assigned structures. The ESI-MS spectra of  
200 compounds **3c** (n = 12) and **7c** show the expected (M – H)<sup>-</sup> and (M - 2H)<sup>2-</sup> ions. The ESI-MS  
201 spectra of **8c** under various conditions are more complex as the monomer ions (M-2H)<sup>2-</sup> co-occur  
202 with dimeric (2M – 4H)<sup>4-</sup> and trimeric (3M – 6H)<sup>6-</sup> ions (Figure 2). The monoisotopic parent  
203 ions of these species occur at the same m/z (804.370) but the differing charges produce different

204 isotopic patterns that allow the species to be identified. This is further evidence of the  
 205 macrocyclic bolaamphiphile structure assigned.



206  
 207 *Scheme 2:* Synthetic routes to nitrophenyl phosphate and nitrobenzoxadiazole phosphate  
 208 derivatized lipid cores.

209  
 210



211

212 *Figure 2.* Isotope distribution patterns of the molecular ions of **8c** aggregates by high-resolution  
 213 ESI-MS (negative ion). Triangles:  $(M-2H)^{2-}$ ; squares:  $(2M-4H)^{4-}$ ; circles:  $(3M-6H)^{6-}$ .

214

215 Alternative lipids required for a fluorescence quenching assay of membrane-spanning proportion

216 (see below) were prepared from the lipid cores **8b**, **7b**, and **3b** using a phosphorodichloridate

217 reagent prepared *in situ* from **11** and  $POCl_3$  followed by pyridine-water hydrolysis to give the

218 nitrobenzoxadiazole lipids (NBD-lipids) **8d**, **7d** and **3d** ( $n = 14$ ) (Scheme 2). The procedure was

219 optimized to utilize reagents in excess to fully convert small amounts of the lipid cores ( $< 10$

220  $\mu$ mole) to the required compounds, in part to deal with the limited amounts of material then

221 available, and in part to deal with the very gummy insoluble products produced when the solvent

222 was removed. The gummy state could not be re-dissolved in organic solvent mixtures after it

223 had formed. Gummy samples could be dispersed into aqueous solution, consistent with the

224 formation of lipid aggregates; these were not further explored. Compound characterization of

225 **8d**, **7d** and **3d** ( $n = 14$ ) rests entirely on the observation of the expected molecular ions in the

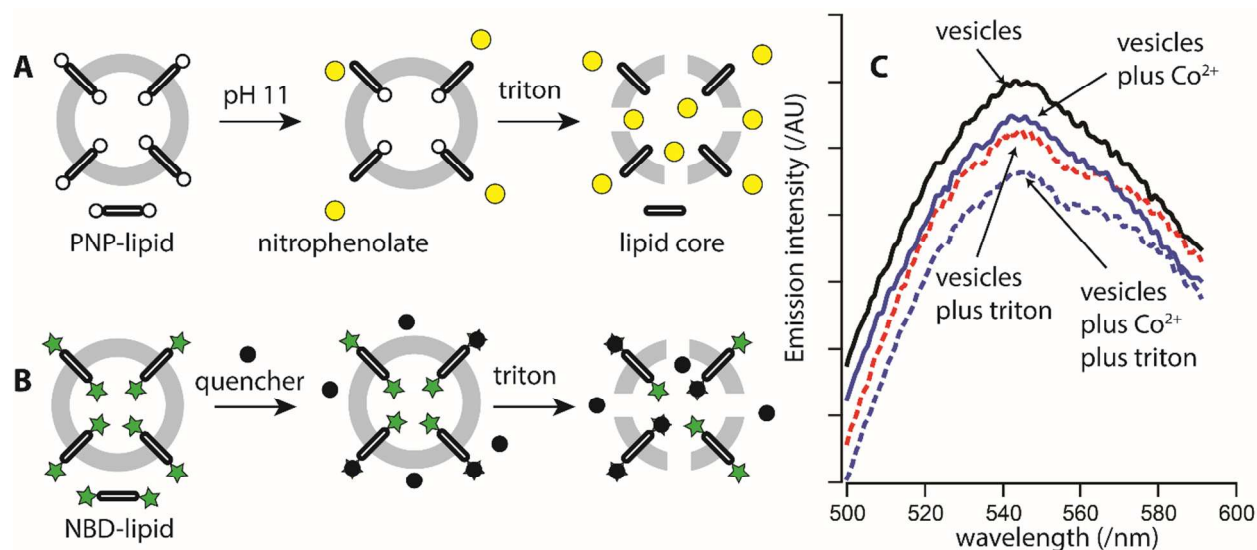
226 ESI-MS (negative ion) spectra of the products produced by the protocol as solutions of 0.1-1 mM  
227 concentration in chloroform, and on the expected UV-visible and fluorescence spectra obtained.

228

### 229 *Determination of membrane-spanning proportion*

230 Determination of membrane-spanning proportion in a bilayer-membrane vesicle requires a  
231 technique to differentiate those head groups of a bolaamphiphile that reside in the outer leaflet  
232 from those located on the inner leaflet. This requires a surface-specific reaction by a membrane-  
233 impermeable reactant (Figure 3A). The pioneering work by Moss and co-workers exploited  
234 base-promoted ester hydrolysis to expose a nitrophenolate ion from the head groups of a single-  
235 strand bolaamphiphile in vesicles composed of quaternary ammonium lipids; a “rapid” phase of  
236 the reaction over the first 100 seconds produced 50% of the eventual (8 hour) total  
237 nitrophenolate produced<sup>45</sup>. This was taken as evidence that the bolaamphiphile was exclusively  
238 membrane-spanning in the initial stages of the reaction. The same strategy of surface-specific  
239 reaction was exploited to create transverse asymmetric lipid distributions<sup>44,46</sup> as a prelude to  
240 examining lipid flop-flop rates. The observation of 50% surface reaction in this type of assay  
241 does not rule out the possibility that the bolaamphiphiles are also inserted as U-shaped within a  
242 single leaflet with equal proportions on the inner and outer leaflets and subsequent control  
243 experiments on flip-flop rates are required to rule out this possibility<sup>45</sup>.

244



245

246

247 *Figure 3.* Assays to assess membrane-spanning proportion by bolaamphiphile lipids. A:  
 248 Schematic of the nitrophenolate release assay<sup>44</sup>. Addition of base results in hydrolysis of  
 249 phosphate esters on the external face of the vesicle to release a portion of the total nitrophenolate  
 250 associated with the vesicle; triton addition results in lysis to expose the internal face of the  
 251 vesicles to the base and results in additional nitrophenolate release. B: Schematic of the NBD-  
 252 quenching assay. Addition of a quencher to the vesicles results in partial quenching of the total  
 253 NBD emission proportional to the fraction of externally bound NBD. Addition of triton results  
 254 in vesicle lysis to expose NBD initially held inside the vesicle and results in quenching of a  
 255 larger proportion of the total emission. C: NBD-emission spectra for vesicles containing **8d** (0.2  
 256 wt%) showing changes due to addition of 0.2 mM CoSO<sub>4</sub> and triton (excess with respect to total  
 257 lipid).

258

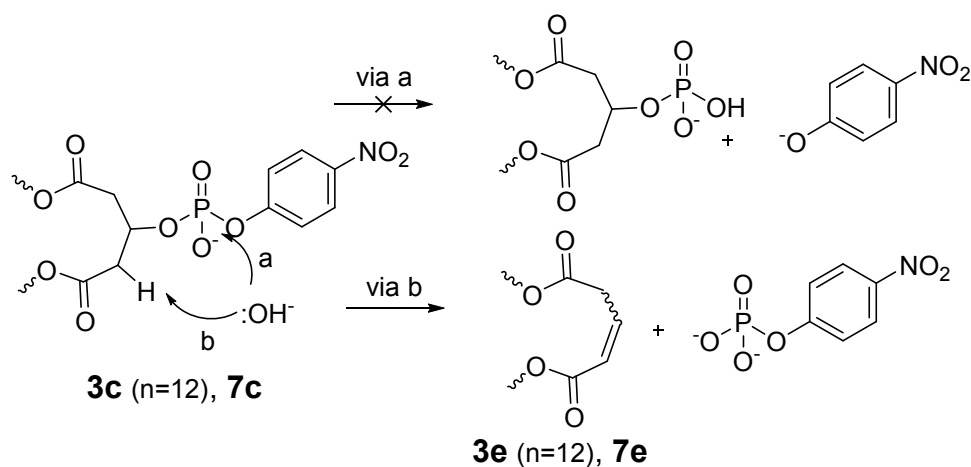
259

260 As discussed above, a commercially available reagent readily converted the lipid cores to  
261 suitable nitrophenylphosphate ester amphiphiles **3c** (n = 12), **7c**, and **8c** needed to utilize the  
262 Moss assay for membrane-spanning proportion<sup>44</sup>. Mixed lipid films of L- $\alpha$ -phosphatidylcholine  
263 containing about 1 mol% of **3c** (n = 12), **7c**, or **8c** were hydrated in a phosphate buffer at pH 6.4,  
264 and vesicles of diameter 125-150 nm were formed using a conventional sequence of cycles of  
265 freeze-thaw, sonication, extrusion sizing, and gel filtration for all three additives. Despite the  
266 apparent incorporation of **3c** (n = 12), **7c**, or **8c** into the vesicles, a shift in pH to 11.8 by addition  
267 of NaOH failed to release any of the expected yellow nitrophenolate ion in any attempt. There are  
268 several possibilities for this disappointing outcome: the synthetic lipids were not taken into the  
269 vesicles during formation or were lost on the gel permeation column; the head group  
270 phosphodiester is unreactive under the conditions of the assay; there is a competing side-reaction  
271 that does not involve formation of nitrophenolate.

272  
273 Uptake of **3c** (n = 12) or **7c** during vesicle formation was readily established. Vesicles were  
274 formed as previously, triton was added to lyse the vesicles and the sample was diluted in methanol  
275 for ESI-MS (negative ion) analysis. In addition to many peaks related to the other components in  
276 this mixture, the expected (M - H)<sup>-</sup> ions of **3c** (n = 12) was observed at *m/z* 684.5 and of **7c** at *m/z*  
277 1454.1 in their respective vesicle samples. Compound **8c** could not be directly detected by this  
278 procedure. As noted above, the observed ions in pure samples include homo-aggregates which  
279 are not present in the complex spectra obtained. We assume that some of the observed ions are  
280 aggregates of **8c** with phosphatidylcholines but there is no unambiguous assignment of the  
281 presence **8c**.

282

283 The stability of **3c** (n = 12) or **7c** under the reaction conditions was assessed using the same direct  
284 ESI-MS analysis of vesicle products following various times of exposure to pH 11.8. We  
285 anticipated a decay of the observed parent ions initially present. Given the complexity of the  
286 spectra and the relatively crude sample preparation method it was difficult to establish if there was  
287 a time-dependent loss of ion intensity; the molecular ions were observed for both systems under  
288 all base treatment times. Both systems did produce new ions on base treatment, and significantly  
289 both systems produced a new ion 219 mass units lower than the parent ( $m/z$  465.9 from 684.8 for  
290 **3c** (n = 12) and  $m/z$  1235.1 from 1454.1 for **7c**). This mass difference corresponds to the loss of  
291 the entire nitrophenyl phosphate head group without cleavage of the nitrophenyl ester. This  
292 suggests that a side-reaction has occurred by elimination as illustrated in Scheme 3. We  
293 expected direct hydrolysis (path following a); we appear to observed elimination (path following  
294 b). A monoanionic species is observed by ESI-MS in both cases. For **7e** we can assume the  
295 remaining phosphate is deprotonated and the  $\alpha,\beta$ -unsaturated ester is a neutral but for **3e** (n = 12)  
296 we require the additional assumption that the  $\alpha,\beta$ -unsaturated ester is  $\gamma$ -deprotonated to form a  
297 delocalized ion along the glutarate-derived strand. We were also able to produce **3e** (n = 12) in a  
298 preparative-scale reaction in a biphasic mixture of dichloromethane-THF with added aqueous  
299 NaOH. The isolated mixture of elimination products showed the expected additional vinylic  
300 signals required for **3e** in the  $^1\text{H-NMR}$  spectrum.



301

302 *Scheme 3:* Proposed competing hydrolysis and elimination of nitrophenyl phosphate during the  
 303 membrane-spanning assay of Fig 3A.

304

305 Although the logic of this (failed) assay is sound, it does have inherent ambiguities related to  
 306 reaction rate relative to either lipid flip-flop or membrane permeation of the reagent. Another  
 307 reaction that has been used in this context is the reduction of nitrobenzoxadiazole (NBD) lipids  
 308 by dithionite<sup>37,47-50</sup>, but this approach would suffer from the same ambiguities. As we thought  
 309 about an alternative head group for the membrane-spanning proportion assay, we noted the early  
 310 papers on the quenching of NBD-lipid fluorescence by  $\text{Co}^{2+}$  and  $\text{Cu}^{2+}$ <sup>47,51</sup>. Since a fluorescence  
 311 quenching assay would not require reaction time after initial mixing, this approach could  
 312 potentially be faster and could provide an *in situ* probe for continuous monitoring of any  
 313 competing processes such as membrane permeation or lipid flip-flop. The proposed assay is  
 314 sketched in Figure 3B; an initially fluorescent vesicle population would suffer partial quenching  
 315 on addition of the quencher to the outside of the vesicles. This would only be partial quenching  
 316 dependent upon the quencher concentration according to a Stern Volmer dependence. Upon  
 317 vesicle lysis with a detergent such as triton, an additional fraction of the fluorescent head groups  
 318 would be quenched. The proportion of membrane-spanning bolaamphiphiles would be related to  
 319 the ratio of the extents of quenching. There are obvious complexities with such an assay. In the

320 version developed, the main issue is that  $\text{Co}^{2+}$  quenching is known to be influenced by vesicle  
321 surface charge and the vesicles themselves are unstable at high  $\text{Co}^{2+}$  concentration<sup>51</sup>. This  
322 requires the lowest possible quencher concentration, thus limiting the assay in the extent of the  
323 quenching that can be achieved. The analysis also needs to contend with the proportion of the  
324 signal that depends on the scattering of both incident and emitted light from the vesicles; any  
325 change to the vesicle morphology or population size-distribution, such as provoked by addition  
326 of the detergent, has the potential to alter this factor and to confound the analysis of the signal  
327 and the ratios required for the determination of membrane-spanning proportion. Yet even if these  
328 technical hurdles of a fluorescence assay prove to be insurmountable, the dithionite reduction  
329 reaction-based assay remains as a potential back-up.

330

331 We therefore prepared NBD-labelled lipid cores **3d** ( $n = 14$ ), **7d**, and **8d** as outlined above. The  
332 synthetic NBD-lipids were handled as dilute solutions with the concentration determined by UV-  
333 visible spectroscopy based on the assumption that the molar absorptivity of the NBD group was  
334 the same as that of **11** ( $\lambda_{\text{max}} 475 \text{ nm}$ ;  $\epsilon 1.82 \times 10^4 \text{ Lmol}^{-1}\text{cm}^{-1}$ ;  $\text{CHCl}_3$ ). From a spectroscopic  
335 perspective all three samples behaved the same as a commercially available NBD-lipid derived  
336 from distearoylphosphatidyl ethanolamine (NBD-DSPE). In particular, the absorbance and the  
337 emission spectra of **3d** ( $n = 14$ ) were essentially superimposable on those of NBD-DSPE at the  
338 same concentration, while solutions of **7d** and **8d** appeared to be twice as concentrated but  
339 preserved the same absorption and emission maxima in  $\text{CHCl}_3$  solution.

340

341 All four NBD-lipids were taken into vesicles comprised of egg phosphatidyl choline (70 wt%),  
342 cholesterol (25 wt%), a polyethyleneglycol derivatized phosphatidyl ethanolamine (3 wt%), and

343 egg phosphatidic acid (2 wt%). The NBD lipids were added to a chloroform solution of the lipid  
344 mixture to give an NBD concentration of 0.08 mol% (about 0.1 wt% for **3d** (n= 14), the solvent  
345 was removed to form a lipid film that was hydrated in a HEPES buffer at pH 7.2, subjected to  
346 five freeze-thaw cycles, sonication, extrusion through a 0.1  $\mu\text{m}$  Nucleopore membrane, and gel  
347 permeation chromatography to remove unbound materials. All NBD-lipids were obviously  
348 incorporated based on the pale yellow color and the green fluorescence under hand-held UV  
349 light. The vesicles had the expected range of sizes between 125 and 200 nm mean diameter  
350 depending on the preparation. Excitation at 470 nm produced a clear fluorescence emission  
351 about 540 nm; the position of the emission maximum was variable between 538 and 545 nm as  
352 has been previously ascribed to differences in the NBD location in the mid-polar region leading  
353 to changes in the contribution of water quenching to the observed emission<sup>47</sup>.

354  
355 Addition of  $\text{CoSO}_4$  quenches the NBD fluorescence of NBD-DSPC in vesicles. In the  
356 concentration range 10 – 50 mM  $\text{Co}^{2+}$  the plot of  $(I_0/I - 1)$  as a function of  $\text{Co}^{2+}$  concentration is  
357 linear ( $r^2 = 0.9977$ ;  $n = 5$ ) with a Stern Volmer quenching constant of  $18.6 \pm 0.5 \text{ M}^{-1}$ . This is in  
358 reasonable agreement with the reported value of  $13.8 \text{ M}^{-1}$  for the same NBD-lipid and  $\text{Co}^{2+}$   
359 concentration range in a vesicle system composed of phosphatidyl serine and phosphatidyl  
360 ethanolamine (1:1)<sup>51</sup>. However, the intercept of the linear fit is greater than zero and the data  
361 below 10 mM in  $\text{Co}^{2+}$  concentration are distinctly curved to zero. This behavior is similar to that  
362 observed in cases where there is restricted access to some of the fluorophores in the sample<sup>52</sup>.  
363 Compound **3d** ( $n = 14$ ) behaves very similarly; above 8 mM  $\text{Co}^{2+}$  the Stern Volmer quenching  
364 constant is  $15.7 \pm 0.5$  ( $r^2 = 0.9957$ ;  $n = 7$  to 40 mM) with an intercept greater than zero. In the  
365 presence of the detergent, triton, in the same  $\text{Co}^{2+}$  concentration range, the Stern Volmer

366 quenching constant is essentially unchanged ( $16.3 \pm 0.4$ ,  $r^2 = 0.9976$ ;  $n = 7$  to 40 mM) but the  
367 intercept is zero within experimental error ( $0.008 \pm 0.009$ ). In the very low concentration range  
368 of 0 – 0.2 mM  $\text{Co}^{2+}$  without added triton, a linear fit produces an apparent Stern Volmer constant  
369 of  $215 \pm 15 \text{ M}^{-1}$  ( $r^2 = 0.98$ ;  $n = 5$ ). Whatever the photophysical origins of these behaviors might  
370 be, they have the positive practical consequence that sufficient quenching can be observed at 0.2  
371 mM  $\text{Co}^{2+}$  concentration to ensure that the quencher concentration lies well below the level at  
372 which transport and aggregation could be significant competitive processes.

373  
374 As encouraging as these results were, there is a technical hurdle to overcome in that the addition  
375 of triton causes an apparent quenching of the emission. Figure 3C shows one example (**8d**) in  
376 which the addition of the detergent causes about the same extent of quenching as the addition of  
377 the quencher  $\text{Co}^{2+}$ . This may be due to a change in vesicle morphology that results in a change  
378 in light scattering, or it may reflect the influence of the detergent on the region where the NBD  
379 fluorophore resides that alters the extent of quenching by water<sup>47</sup>. As shown in Figure 3C the  
380 addition of  $\text{Co}^{2+}$  to vesicles already treated with triton results in additional quenching, shown  
381 above to occur with the same efficiency as in the absence of the detergent. We reasoned that the  
382 Stern Volmer factors ( $I_0/I-1$ ) in the absence of triton would be proportional to the fraction of  
383 NBD in the outer leaflet only, while the same factor in the presence of detergent would be  
384 proportional to the total NBD in the system. Thus the ratio of the Stern Volmer factors in the  
385 absence and in the presence of triton gives a measure of the proportion of the NBD head groups  
386 that lie in the outer leaflet. In the case of **3d** ( $n = 14$ ) this ratio is  $0.52 \pm 0.03$  for three trials from  
387 the same vesicle population. This is the expected value. As a dilute dopant **3d** should be equally  
388 distributed in each leaflet but the outer leaflet has a slightly larger area than the inner leaflet

389 making the outer area 53% of the total area (based on the experimentally determined vesicle  
390 diameter of 132 nm with an assumed 4 nm membrane thickness). We therefore conclude that  
391 our procedure correctly estimates the outer leaflet proportion of NBD head groups.

392  
393 The spectra obtained for similar experiments with vesicles containing the bolaamphiphiles **8d**  
394 (Fig. 3C) or **7d** “look” the same but differ significantly in the level of the head group proportion  
395 apparently in the outer leaflet: **7d** gives an outer leaflet head group proportion of  $0.75 \pm 0.03$   
396 while **8d** gives  $0.48 \pm 0.04$ . Note that in both these cases the expectation value for a membrane-  
397 spanning bolaamphiphile is 50% as the outer proportion does not depend on vesicle curvature.  
398 The experimental value for **8d** is clearly in line with the expectation that it adopts a membrane-  
399 spanning orientation as a low-level dopant in a predominantly phospholipid bilayer vesicle. The  
400 case of **7d** is much less clear; it is possible that it adopts a U-shaped insertion in a single leaflet  
401 of the phospholipid bilayer, but that would also require the assumption that it is predominantly  
402 located in the outer leaflet. There may be a lipid-packing argument to buttress this assumption as  
403 the outer leaflet lipids occupy a larger area per molecule due to curvature<sup>53</sup> but this would be an  
404 unusually asymmetric distribution between the leaflets more commonly associated with small  
405 vesicles of higher curvature<sup>54</sup>. Alternatively, the U-shaped insertion might enhance the  
406 membrane permeability to  $\text{Co}^{2+}$  via defects as has previously been found in the synthetic ion  
407 channels area<sup>18-20</sup>. If permeation of  $\text{Co}^{2+}$  occurs, it could result in a time-dependent signal in the  
408 absence of triton; this was not observed in any experiment involving **3d** ( $n = 14$ ), **7d**, or **8d** over  
409 time spans to 20 minutes suggesting that the quenching behavior reaches a steady value within  
410 the mixing and sample preparation time (less than 1 minute). Whatever the explanation, the  
411 conclusion from the experiments is that **7d** does not produce a solely membrane-spanning

412 orientation at low concentration in phospholipid bilayers; if it did, it would have approximated  
413 the experimental result for **8d**.

414

## 415 **Conclusions**

416 The synthesis of a 72-membered macrocyclic tetraester bolaamphiphile was readily  
417 accomplished in a short sequence from commercially available starting materials using CuAAC.

418 The 87% yield in the final macrocyclization step played a major role in the overall 26% yield in  
419 five steps to the lipid core diol. Subsequent losses occurred as phosphate head groups were  
420 appended but the methods reported produce the macrocyclic lipids in acceptable overall yields.

421 Lipids with two different phosphate head groups readily incorporated into phospholipid vesicles  
422 as directly detected in the NBD-lipid case or by ESI-MS analysis in the case of nitrophenyl  
423 phosphate lipids. Unfortunately the latter failed to undergo phosphate hydrolysis under basic  
424 conditions, rather undergoing elimination in competition, so could not be used to assay

425 membrane-spanning proportion. The NBD-lipids produced allowed a new assay for membrane-  
426 spanning proportion to be explored based on the quenching of NBD fluorescence by cobalt ions.

427 Apparent quenching in the presence of triton as detergent requires the comparison of the Stern  
428 Volmer factors in the absence and presence of the detergent. The macrocyclic bolaamphiphile

429 **8d** is incorporated into phospholipid vesicles such that  $48 \pm 4\%$  of the NBD head groups are in  
430 the outer leaflet, consistent with a membrane-spanning orientation. There is no time-dependent

431 change in quenching over 20 minutes, indicating that **8d** does not significantly alter the

432 membrane permeability to the quencher or undergo lipid reorganization in this time scale. The

433 acyclic bolaamphiphile **7d** is incorporated with  $75 \pm 3\%$  of the NBD head groups accessible to

434 quencher in the absence of a detergent suggesting U-shaped incorporation in the outer leaflet of  
435 the bilayer membrane and/or some induced permeability of the vesicles by **7d**.

436  
437 To what extent is the lipid core **8b** a mimic of the caldarchaeols? On a trivial level they both  
438 contain 72-membered rings and **8b** derived lipids incorporate well into vesicles in a membrane-  
439 spanning orientation in line with the behavior of archaeal lipids. On the other hand **8b** has  
440 completely different chemical functionality and any presumed mechanical advantage of **8b**-  
441 derived lipids in stabilizing bilayer membranes has yet to be explored. In fairness, the functional  
442 role of the natural macrocycle is only indirectly inferred. All that can be stated at this point is  
443 that other derivatives of this mimic offer the potential to explore specific hypotheses and may  
444 lead to clarification of the roles of macrocyclic archaeal lipids.

445

## 446 **Experimental**

### 447 *Synthesis:*

#### 448 *General procedure for preparation of glutarate monoesters: 2, 4*

449 In a 2 necked round bottom flask a stirred solution in toluene (19 mL) was prepared from 3-  
450 (*tert*- butyl dimethylsilyloxy) glutaric anhydride (1.15 equiv.) and the alcohol (1.00 equiv.). The  
451 reaction mixture was set to stir at reflux for 24 hours under a CaSO<sub>4</sub> drying tube. The reaction  
452 was monitored by TLC (silica gel, EtOAc/Hexanes as eluent, visualized by KMnO<sub>4</sub>). Once  
453 complete, the reaction was cooled and toluene evaporated at reduced pressure. The crude  
454 product was then redissolved in pentane and cooled in a dry ice ethanol bath then vacuum  
455 filtered. Crystallization of excess anhydride from the filtrate was repeated until the excess

456 crystals no longer formed. If alcohol impurities existed, as visualized by NMR, the crude  
457 product was purified by column chromatography on silica gel, using EtOAc/Hexanes as eluent.  
458 The following compounds were prepared by this procedure:

459 **2** (n = 12) from 1-dodecanol (0.780 mL, 4.07 mmol) as a colourless oil in 95% yield  
460 (1.655 g). <sup>1</sup>H-NMR (300 MHz, CDCl<sub>3</sub>) δ: 4.54 (q, 1H, J=6.0 Hz), 4.06 (dt, 2H, J=1.5, 6.9 Hz),  
461 2.70-2.55 (m, 4H), 1.64-1.26 (m, 20H), 0.90-0.87 (m, 12H), 0.10 (s, 3H), 0.09 (s, 3H). <sup>13</sup>C-  
462 NMR (75MHz, CDCl<sub>3</sub>) δ: 177.0, 171.1, 67.9, 66.2, 64.8, 42.5, 42.4, 32.0, 29.7, 29.6, 29.5, 29.4,  
463 29.3, 28.6, 26.0, 25.7, 22.7, 17.9, 14.1, -4.87, -4.92. ESI-MS (-ve): calc'd for C<sub>23</sub>H<sub>45</sub>O<sub>5</sub>Si (M-H<sup>-</sup>)  
464 ), 429.304 amu; found, 429.306 amu.

465 **2** (n = 14) from 1-tetradecanol (1.140 g, 4.665 mmol) in 53% yield (1.397 g). <sup>1</sup>H NMR  
466 (300 MHz, CDCl<sub>3</sub>) δ: 4.54 (quin, 1H, J=6 Hz), 4.12-3.99 (m, 2H), 2.67-2.52 (m, 4H), 1.66-1.18  
467 (m, 24H), 0.90-0.83 (m, 12H), 0.072 (s, 3H), 0.066 (s, 3H). <sup>13</sup>C NMR (300 MHz, CDCl<sub>3</sub>) δ:  
468 176.5, 171.0, 66.1, 64.8, 42.4, 42.2, 31.9, 29.65, 29.61, 29.54, 29.46, 29.3, 29.2, 28.5, 25.9,  
469 25.8, 22.7, 17.8, 14.1, -4.9, -5.0. ESI-MS (-ve): calc'd for C<sub>25</sub>H<sub>49</sub>O<sub>5</sub>Si (M-H<sup>-</sup>), 457.366 amu;  
470 found, 457.374 amu.

471 **4** from 10-undecyn- 1-ol (1.49 mL, 7.77 mmol) in 87% yield (2.78 g). <sup>1</sup>H-NMR (300  
472 MHz, CDCl<sub>3</sub>) δ: 4.54 (q, 1H, J=6.0 Hz), 4.06 (dt, 2H, J=6.9, 1.5 Hz), 2.7-2.54 (m, 4H), 2.19  
473 (dt, 2H, J=2.7, 6.9 Hz), 1.93 (t, 1H, J=3.0 Hz), 1.25-1.66 (m, 14H), 0.86 (s, 9H), 0.09 (s, 3H),  
474 0.08 (s, 3H). <sup>13</sup>C-NMR (75 MHz, CDCl<sub>3</sub>) δ: 177.0, 171.0, 84.6, 68.1, 66.1, 64.7, 42.4, 42.2,  
475 30.3, 29.6, 29.3, 29.1, 28.9, 28.6, 28.5, 28.4, 25.8, 25.6, 18.3, 17.8, -4.9, -5.0. ESI-MS (-ve):  
476 calc'd for C<sub>22</sub>H<sub>39</sub>SiO<sub>5</sub> (M-H<sup>-</sup>), 411.256 amu; found, 411.257 amu.

477

478 *General procedure for preparation of glutarate diesters: 3a, 7a*

479 The glutarate monoester (1.0 equiv.) was dissolved in dry THF(15 mL). Under a flow of N<sub>2</sub>  
480 DIC (1.5 equiv.) was added and stirred for 5 minutes. HOBt(1.5 equiv.) was then added and  
481 stirred for 5 minutes, followed by the alcohol (1.5 equiv.) which was stirred for 5 minutes,  
482 followed by DiPEA( 3.0 equiv.). The reaction was left stirring at r.t. for 3 hours. The reaction  
483 was then vacuum filtered and the filtrate concentrated. The product was then dissolved in 50  
484 mL DCM and extracted two times with H<sub>3</sub>PO<sub>4</sub>/ NaH<sub>2</sub>PO<sub>4</sub> buffer solution (50 mL, pH~3), two  
485 times with Na<sub>2</sub>HPO<sub>4</sub>/ NaH<sub>2</sub>PO<sub>4</sub> buffer solution (50 mL, pH~7), one time with water (50 mL),  
486 two times with 10% brine solution (50 mL), and finally washed once with a saturated solution  
487 of NaCl (50 mL). The crude waxy product was washed with MeOH, the resulting solution was  
488 vacuum filtered. The MeOH wash was repeated as many times as necessary to increase purity  
489 as assessed by NMR with concomitant loss of yield.

490 **3a** (n =12) from 1-dodecanol and **2** (n = 12) (1.270 g, 2.958 mmol) 70% yield (1.238  
491 g). <sup>1</sup>H- NMR (300 MHz, CDCl<sub>3</sub>) δ: 4.52 (q, 1H, J=6.0 Hz), 4.06-4.01 (m, 4H), 2.52 (d, 4H,  
492 J=6.3 Hz) 1.62-1.24 (m, 40H), 0.88-0.82 (m, 15H), 0.82 (s, 9H), 0.04 (s, 6H). <sup>13</sup>C-NMR (75  
493 MHz, CDCl<sub>3</sub>) δ: 171.2, 66.5, 64.8, 42.7, 32.0, 29.8, 29.7, 29.6, 29.5, 29.4, 28.7, 26.1, 25.8,  
494 22.8, 18.0, 14.2, -4.8. ESI-MS (+ve): calc'd for C<sub>35</sub>H<sub>71</sub>O<sub>5</sub>Si (M+H<sup>+</sup>), 599.5065 amu; found,  
495 599.5065 amu.

496 **3a** (n=14) from 1-tetradecanol (1.101 g, 2.399 mmol) 59% yield (0.8524 g, 1.422 mmol).  
497 <sup>1</sup>H NMR (300 MHz, *d*<sub>6</sub>-acetone) δ: 4.59 (quin, 1H, J=6 Hz), 4.13-3.99 (m, 4H), 2.63-2.50 (m,  
498 4H), 1.68-1.28 (m, 48H), 0.91-0.86 (m, 15H), 0.093 (s, 6H). <sup>13</sup>C NMR (300 MHz, *d*<sub>6</sub>-acetone) δ:  
499 171.4, 67.5, 65.0, 43.1, 33.9, 32.8, 30.5, 30.4, 30.1, 29.5, 26.8, 26.3, 23.4, 18.6, 14.5, -4.5. ESI-  
500 MS (+ve): calc'd for C<sub>39</sub>H<sub>79</sub>O<sub>5</sub>Si (M+H<sup>+</sup>), 655.569 amu; found, 655.565 amu.

501 **7a** from **6** (1.663 g, 1.694 mmol) and 10-undecyn-1-ol(0.780 mL, 4.06 mmol). The crude  
502 product was purified by column chromatography on silica gel, using EtOAc/hexanes as eluent  
503 affording a colourless oil 43% yield (0.930 g). <sup>1</sup>H- NMR (300 MHz, CDCl<sub>3</sub>) δ: 7.18 (s, 2H), 4.50  
504 (q, 2H, J=6.3 Hz), 4.42 (t, 2H, J=5.1 Hz), 4.04-3.98 (m, 8H) 3.78 (t, 2H, J=4.8 Hz), 2.65 (t, 4H,  
505 J=7.8 Hz), 2.51 (d, 8H, J=6.3 Hz), 2.14 (dt, 4H, J=2.7, 6.9 Hz), 1.90 (t, 2H, J=2.7 Hz) 1.64-1.22  
506 (m, 56H), 0.80 (s, 18) 0.02 (s, 12H). <sup>13</sup>C- NMR (75 MHz, CDCl<sub>3</sub>) δ: 171.2, 148.6, 121.4, 84.8,  
507 69.6, 68.2, 64.7, 50.0, 42.7, 29.6, 29.5, 29.4, 29.3, 29.25, 29.1, 28.8, 28.7, 28.5, 26.0, 25.9, 25.8,  
508 25.76, 18.5, 18.0, -4.8. ESI- MS (+ve): calc'd for C<sub>70</sub>H<sub>125</sub>N<sub>6</sub>Si<sub>2</sub>O<sub>11</sub> (M+H<sup>+</sup>), 1281.894 amu;  
509 found, 1281.893 amu.

510

511 *General procedure for TBDMS deprotections: 3b, 7b, 8b*

512 The TBDMS protected glutarate diester (1.0 equiv.) was placed in a round bottom flask.  
513 TBAF (5.80 mL, 5.8 mmol, 5.0 equiv. from a 1.0 M stock solution in THF), was added  
514 concurrently with AcOH (3.30 mL, 1.45 mmol, 1.25 equiv. from a 0.438 M stock solution in  
515 THF). The solution was stirred under N<sub>2</sub> for 30 minutes at r.t. while being monitored by  
516 NMR. When the reaction was complete it was quenched with a saturated NH<sub>4</sub>Cl solution and  
517 DCM (25 mL) was added. The organic layer was washed with water (25 mL), brine (25 mL),  
518 and finally dilute acid (25 mL water, 2 drops HCl). The solvent was dried with Na<sub>2</sub>SO<sub>4</sub>,  
519 vacuum filtered and the solvent removed under reduced pressure. The crude product was  
520 dissolved in pentane (25 mL) and crystallized in an ethanol/dry ice bath.

521 **3b** (n = 12) was prepared from **3a** (n = 12) (0.6900 g, 1.15 mmol) 90% yield (502  
522 mg). <sup>1</sup>H-NMR (300 MHz, CDCl<sub>3</sub>) δ: 4.44 (q, 1H, J=6.3 Hz), 4.09 (t, 4H, J=6.6 Hz), 3.41 (s,  
523 1H), 2.53 (d, 4H, J=6.3 Hz), 1.64-1.25 (m, 40H), 0.87 (t, 6H, J=6.2 Hz). <sup>13</sup>C- NMR (75 MHz,

524 CDCl<sub>3</sub>) δ: 172.0, 65.1, 64.9, 40.8, 32.0, 29.72, 29.67, 29.6, 29.4, 29.3, 28.7, 26.0, 22.8, 14.2.

525 ESI-MS (+ve): calc'd for C<sub>29</sub>H<sub>57</sub>O<sub>5</sub> (M+H<sup>+</sup>), 485.4200 amu; found, 485.4199 amu.

526 **3b** (n = 14) was prepared from **3a** (n = 14) (0.248 g, 0.395 mmol) 35% (0.0749 g,

527 0.139 mmol). <sup>1</sup>H NMR (300 MHz, CDCl<sub>3</sub>) δ: 4.43 (quin, 1H, J=6 Hz), 4.08 (t, 4H, J=7 Hz),

528 2.53 (d, 4H, J=6 Hz), 1.30-1.24 (m, 48H), 0.86 (t, 6H, J=7 Hz). δ: 3.37-3.31 (m, 2H), 1.63-

529 1.58 (m, 4H), 1.47-1.40 (m, 2H), 0.99 (t, 3H, J=7 Hz). <sup>13</sup>C NMR (300 MHz, CDCl<sub>3</sub>) δ: 171.8,

530 64.9, 64.8, 40.7, 31.9, 29.6, 29.52, 29.46, 29.3, 29.2, 28.5, 25.8, 22.6, 14.0. ESI-MS (+ve):

531 calc'd for C<sub>33</sub>H<sub>65</sub>O<sub>5</sub> (M+H<sup>+</sup>), 541.483 amu; found, 541.484 amu.

532 **7b** was prepared from **7a** (271 mg, 0.211 mmol), as a white solid 68% yield (152 mg).

533 <sup>1</sup>H- NMR (300 MHz, CDCl<sub>3</sub>) δ: 7.16 (s, 2H), 4.40 (m, 6H), 4.03 (t, 8H, J=6.8 Hz), 3.75 (t, 4H,

534 5.1 Hz), 3.52 (s, 2H), 2.62 (t, 4H, 7.5 Hz), 2.49 (d, 8H, J=6.3 Hz), 2.11 (dt, 4H, J=2.7, 6.9 Hz),

535 1.88 (t, 2H, 2.7 Hz), 1.58-1.24 (m, 56H). <sup>13</sup>C- NMR (75 MHz, CDCl<sub>3</sub>) δ: 171.8, 148.4, 121.4,

536 84.7, 69.5, 68.2, 64.9, 64.8, 49.9, 40.8, 29.5, 29.4, 29.3, 29.14, 29.13, 29.0, 28.7, 28.5, 25.8,

537 25.6, 22.7, 18.4. ESI- MS (+ve): calc'd for C<sub>58</sub>H<sub>97</sub>N<sub>6</sub>O<sub>11</sub> (M+H<sup>+</sup>), 1053.721 amu, found,

538 1053.720 amu.

539 **8b** was prepared from **8a** (93.2 mg, 0.0638 mmol) as a white solid 86% yield (77.2 mg).

540 <sup>1</sup>H- NMR (300 MHz, CDCl<sub>3</sub>) δ: 7.21-7.17 (m, 4H), 4.43-4.46 (m, 10H), 4.08 (t, 8H, J=6.9 Hz),

541 3.80 (t, 8H, J=5.1 Hz), 3.54 (s, 2H), 2.67 (t, 8H, J=8.1 Hz), 2.53 (d, 8H, J=6.3 Hz), 1.13-1.63 (m,

542 56H). <sup>13</sup>C- NMR (75 MHz, CDCl<sub>3</sub>) δ: 172.0, 148.6, 121.5, 69.6, 65.0, 64.9, 50.0, 40.9, 29.6,

543 29.5, 29.4, 29.3, 28.7, 26.0, 25.8. ESI-MS (+ve): calc'd for C<sub>62</sub>H<sub>105</sub>N<sub>12</sub>O<sub>12</sub> (M+H<sup>+</sup>), 1209.796

544 amu, found, 1209.795 amu.

545

546 *Copper catalyzed azide-acetylene couplings: 6, 8a*

547 **6** was prepared from **4** (1.612 g, 3.920 mmol, 1.99 equiv.), and DMAP (0.039 g, 0.32 mmol, 0.16  
548 equiv.) dissolved in a stirred solution in DMF (32 mL). The azide 1,1'-oxybis(2-azidoethane) (**5**,  
549 0.308 g, 1.97 mmol, 1.00 equiv.) was added and the solution was degassed for 20 minutes with  
550 N<sub>2</sub>, and then CuI (0.186 g, 0.977 mmol, 0.496 equiv.) was added. The flask was flushed with N<sub>2</sub>  
551 and then sealed under a positive pressure of N<sub>2</sub> and stirred for 21.5 hours at 12°C. The reaction  
552 solution was diluted with DCM, and washed with a saturated solution of disodium EDTA  
553 solution (50 mL) until the aqueous layer no longer remained blue. This was followed by two  
554 washes of water (50 mL), and two washes of dilute acid (50 mL, 2 drops 1M HCl). In general no  
555 purification was necessary. If excess azide was present (NMR) the partially reacted product was  
556 removed by dissolving the crude product in EtOAc (2 mL) and precipitated in hexanes (25 mL).  
557 The insoluble material was filtered and the filtrate was concentrated. Washes were repeated until  
558 no impurities remained. The reaction afforded a colourless, tacky semi-solid that retained  
559 solvents that were removed on high vacuum. Compound **6** was a colourless oil afforded in 86%  
560 yield (1.667 g). <sup>1</sup>H-NMR (300 MHz, CDCl<sub>3</sub>) δ: 7.20 (s, 2H), 4.55 (q, 2H, J=6.0 Hz), 4.46 (t, 2H,  
561 J=4.8 Hz), 4.08 (t, 4H, J=6.0 Hz), 3.81 (t, 2H, J=4.8 Hz), 2.68 (t, 4H, J=8.4 Hz), 2.61-2.58 (m,  
562 8H) 1.66-1.25 (m, 28H) 0.85 (s, 18H), 0.09 (s, 6H), 0.08 (s, 6H). <sup>13</sup>C- NMR (125 MHz, CDCl<sub>3</sub>)  
563 δ: 175.0, 171.2, 148.5, 121.9, 69.5, 66.4, 64.8, 50.2, 42.8, 42.5, 29.6, 29.4, 29.3, 29.2, 29.1, 28.6,  
564 26.0, 25.5, 18.0, -4.7, -4.8. ESI-MS (+ve): calc'd for C<sub>48</sub>H<sub>89</sub>N<sub>6</sub>Si<sub>2</sub>O<sub>11</sub> (M+H<sup>+</sup>), 981.6122 amu;  
565 found, 981.6121 amu.

566 **8a** was prepared from **7a** (0.371 g, 0.289 mmol, 1.00 equiv.) and DMAP (0.0025 g,  
567 0.0020 mmol, 0.071 equiv.) in a stirred solution in DMF (2.550 mL) This was followed by 1,1'-  
568 oxybis(2-azidoethane)(0.0452 g, 0.289 mmol, 1.00 equiv.). Conditions and workup as described  
569 for **6**. A colourless solid was afforded in an 87% yield (0.307 g) without need for

570 chromatography.  $^1\text{H-NMR}$  (300 MHz,  $\text{CDCl}_3$ )  $\delta$ : 7.21-7.18 (m, 4H), 7.18 (s, 1H), 4.52 (q, 2H,  
571  $J=6.3\text{Hz}$ ), 4.44 (t, 8H,  $J=5.1\text{ Hz}$ ), 4.06-4.00 (m, 8H), 3.79 (t, 8H,  $J=5.1\text{ Hz}$ ), 2.66 (t, 8H,  $J=7.8$   
572 Hz), 2.52 (d, 8H, 5.7 Hz), 1.66-1.23 (m, 56H), 0.82 (s, 18H), 0.04 (s, 12H).  $^{13}\text{C-NMR}$  (125  
573 MHz,  $\text{CDCl}_3$ )  $\delta$ : 171.24, 171.19, 148.58, 148.54, 121.51, 121.48, 69.62, 69.58, 66.5, 64.78,  
574 64.75, 50.0, 42.7, 29.8, 29.64, 29.55, 29.43, 29.35, 29.3, 28.7, 26.0, 25.8, 18.0, -4.8. ESI-MS  
575 (+ve): calc'd for  $\text{C}_{74}\text{H}_{132}\text{N}_{12}\text{Si}_2\text{O}_{12}\text{Na}$  ( $\text{M}+\text{Na}^+$ ), 1459.951 amu, found, 1459.9542 amu.

576

577 *General procedure for nitrophenyl phosphate lipids: 3c, 7c, 8c*

578 An oven baked round bottom flask was capped and cooled to r.t. under  $\text{N}_2$  and 4-nitrophenyl  
579 phosphorodichloridate (**10**, 6.0 equiv.) was added followed by dry DCM (700 ul) and pyridine  
580 (12 equiv.). The mixture was then stirred for 30 minutes. A second oven baked round bottom  
581 flask and condenser was concurrently cooled under  $\text{N}_2$  to r.t. and the alcohol (1.0 equiv.) was  
582 added followed by dry DCM (100 uL). The **10** / pyridine solution was added dropwise and the  
583 mixture was stirred at r.t. for 30 minutes followed by 7.5 hours at reflux. The reaction was  
584 cooled and  $\text{Et}_2\text{O}:\text{H}_2\text{O}$  (200 uL, 50:50) was added at  $0^\circ\text{C}$ . Following vigorous overnight stirring  
585 the yellow/orange precipitate in the round bottom flask was isolated by decanting the  
586 supernatant and then dissolving the solid in DCM:MeOH (4 mL, 95:5). The product was  
587 precipitated from the solution with water (2 mL) and the precipitate was washed with dilute acid  
588 (2 mL  $\text{H}_2\text{O}$ , 1 drop HCl), and washed again with water (2 mL). The dissolution-precipitation  
589 cycle could be repeated as required. If necessary the product was then adsorbed from  
590 DCM:MeOH onto silica gel and a short column was done with DCM:MeOH eluent to remove  
591 insoluble material, affording a yellow solid after solvent removal, usually with very significant  
592 losses on the column.

593 **3c** (n=12) was prepared from **3b** (n = 12) (50 mg, 0.10 mmol), 32% yield (22.6 mg). <sup>1</sup>H-  
594 NMR (300 MHz, CDCl<sub>3</sub>) δ: 8.14 (d, 2H, J=9 Hz), 7.36 (d, 2H, 8.7 Hz), 5.16 (s, 1H), 3.98-3.95  
595 (m, 4H), 2.82-2.66 (m, 4H), 1.51-1.22 (m, 40H), 0.87 (t, 3H, J=6.3 Hz). <sup>13</sup>C-NMR (125 MHz,  
596 CDCl<sub>3</sub>): 170.9, 125.5, 120.7, 65.7, 39.9, 32.1, 29.82, 29.76, 29.7, 29.50, 29.45, 28.58, 26.0,  
597 22.8, 14.2. ESI-MS (-ve): calc'd for C<sub>35</sub>H<sub>60</sub>NO<sub>10</sub>P (M-H<sup>-</sup>), 684.3881 amu; found, 684.3865  
598 amu.

599 **7c** was prepared from **7b** (95.5 mg, 0.091 mmol,) 17% yield (22.4 mg). <sup>1</sup>H-NMR (300  
600 MHz, CDCl<sub>3</sub>) δ: 7.99 (d, 4H, J=8.4 Hz), 7.17 (s, 4H), 5.13 (s, 2H), 4.84-4.45 (m, 4H) 4.11-  
601 4.04 (m, 12H), 2.68-2.54 (m, 12H), 2.16 (dt, 4H, J=2.7, 6.9 Hz), 1.92 (t, 2H, J=2.7 Hz) 1.64-  
602 1.22 (m, 56H). <sup>13</sup>C-NMR (125 MHz, DMF-d<sub>7</sub>): 171.6, 148.4, 142.8, 125.9, 123.0, 121.2,  
603 85.4, 71.0, 70.1, 65.1, 50.5, 40.8, 26.7, 18.9. ESI- MS (-ve): calc'd for C<sub>70</sub>H<sub>102</sub>N<sub>8</sub>O<sub>21</sub>P<sub>2</sub> (M-  
604 2H<sup>2-</sup>), 726.332 amu; found, 726.330.

605 **8c** was prepared from **8b** (124 mg, 0.10 mmol) 20% yield (33.0 mg). <sup>1</sup>H-NMR (300  
606 MHz, DMSO-d<sub>6</sub>) δ: 8.108-8.083 (m, 4H), 7.59 (s, 4H), 7.32 (s, 4H), 4.74 (s, 2H), 4.41 (s, 8H),  
607 3.82 (s, 8H), 3.74 (s, 8H), 2.71 (s, 8H), 2.53 (s, 8H), 1.52-1.19 (m, 56H). <sup>13</sup>C-NMR (125 MHz,  
608 DMSO-d<sub>6</sub>) δ: 170.0, 146.7, 124.9, 121.9, 119.9, 68.5, 63.8, 49.0, 29.0, 28.9, 28.71, 28.67, 28.6,  
609 27.9, 25.3, 25.0. ESI-MS (-ve): calc'd for C<sub>74</sub>H<sub>110</sub>N<sub>14</sub>O<sub>22</sub>P<sub>2</sub> (M-2H<sup>2-</sup>) 804.370 amu; found,  
610 804.370 amu.

611  
612 *Elimination reaction: NMR sample of 3e*

613 In a round bottom flask **3c** (15 mg, 0.022 mmol, 1.0 equiv.) was dissolved in DCM (2.5 mL)  
614 diluted with THF (20 mL) and 1 M NaOH (145 ul, 0.1 mmol, 7 equiv.) was added with stirring.  
615 After 4 hours at r.t. the reaction mixture was yellow and bleached when acidified with 1 M HCl

616 ( $6.0 \times 10^1$  uL, 0.06 mmol, 3 equiv.). The majority of the solvent (~90%) was removed under  
617 vacuum, extracted with DCM (5 mL), and the organic layer was washed with water (5 mL),  
618 dilute acid (5 mL H<sub>2</sub>O, 1 drop HCl), and again with H<sub>2</sub>O (5 mL). The resulting product was  
619 chromatographed on silica gel with hexanes/ EtOAc to produce a mixed products fraction (~3  
620 mg). <sup>1</sup>H-NMR (300 MHz, CDCl<sub>3</sub>) δ: 7.00 (dt, 1H, J=7.2, 15.6 Hz), 5.93 (dt, 1H, J=1.5, 15.6  
621 Hz), 4.21-4.08 (m, 4H), 3.22 (dd, 2H, J=1.5, 7.2 Hz), 1.64-1.259(m, 40H), 0.87 (t, 3H, J=6.3  
622 Hz).

623

624 *2-(7-nitrobenzofurazan-4-yl)-amino-1-ethanol 11*

625 4-chloro-7-nitrobenzofurazan (1.00 g, 5.01 mmol, 1 eq.) was heated in 35 mL methanol to fully  
626 dissolve the solid. A solution of 2-aminoethanol (2.137 g, 34.99 mmol, 7 eq.) in 8 mL of  
627 methanol was added dropwise and the mixture was held at reflux for 3 hours. Solvent was  
628 removed under reduced pressure to yield a dark orange oil (3.611 g). The product adsorbed on  
629 25g of silica, slurried in 35 mL 15% methanol in chloroform and transferred to a silica column I  
630 the same solvent. Isocratic elution and evaporation gave a product containing trace ethanol  
631 amine which was recrystallized (acetone-hexane) to give NBD-ethanolamine as a red-orange  
632 solid in 39% yield (0.4450 g, 1.985 mmol). <sup>1</sup>H NMR (300 MHz, *d*<sub>6</sub>-acetone) δ: 8.52 (d, 1H, J=9  
633 Hz), 8.14 (br s, 1H), 6.52 (d, 1H, J=9 Hz), 4.23 (br s, 1H), 3.94 (t, 2H, J=5 Hz), 3.78 (br s, 2H).  
634 UV-Vis: λ<sub>max</sub>=475 nm, ε (475 nm, MeOH) = 18200 Lmol<sup>-1</sup>cm<sup>-1</sup>.

635

636 *General procedure for NBD-lipids: 3d, 7d, 8d*

637 Stock solutions: NBD-ethanolamine stock (0.56 g in 10 mL dry THF, 0.25 M), POCl<sub>3</sub> stock  
638 (0.232 mL in 10 mL dry THF, 0.25 M), pyridine/water stock (0.202 mL pyridine + 20 μL water  
639 in 10 mL dry THF, 0.25 M).

640 To 2 mL THF at 80°C under nitrogen was added NBD-ethanolamine stock (0.24 mL, 60 μmol)  
641 and POCl<sub>3</sub> stock (0.24 mL, 60 μmol). The mixture was stirred at reflux for 4 hours and the  
642 alcohol (less than 10 μmol) dissolved in 0.2 mL dry THF was added. After a further 4 hours at  
643 reflux the pyridine/water stock (0.30 mL, 75 μmol) was added and the mixture of solids and  
644 solution was allowed to reflux overnight. The mixture was cooled, solvents were removed under  
645 vacuum, and the solid mass was suspended in 1 mL of CHCl<sub>3</sub> for transfer to a small silica gel  
646 column (40 x8 mm). Elution with CHCl<sub>3</sub> (4 mL) followed by 4 mL each of 0.5% and 1% MeOH

647 in CHCl<sub>3</sub> mobilized an intensely fluorescent band that was collected and concentrated to provide  
648 a stock solution for vesicle experiments. The NBD concentration of the stock was determined by  
649 UV-vis spectroscopy assuming the extinction coefficient of the products was the same as the  
650 starting NBD-ethanolamine. TLC (silica, 10% MeOH in CHCl<sub>3</sub>, R<sub>f</sub> 0.35) established the  
651 presence of a single component in the product solution. ESI-MS (-ve; unit resolution) gave the  
652 expected molecular ions:

653 **3d** calc'd for C<sub>41</sub>H<sub>70</sub>O<sub>11</sub>N<sub>4</sub>P (M-H<sup>-</sup>), 825.5, 826.5 (2:1 ratio); found, 825.5, 826.5 (2.2:1 ratio);

654 **7d** calc'd for C<sub>74</sub>H<sub>108</sub>O<sub>23</sub>N<sub>14</sub>P<sub>2</sub> (M-2H<sup>2-</sup>), 811.36, 811.86 (1.2:1 ratio); found, 811.25, 811.8 (1:1  
655 ratio);

656 **8d** calc'd for C<sub>78</sub>H<sub>116</sub>O<sub>24</sub>N<sub>20</sub>P<sub>2</sub> (M-2H<sup>2-</sup>), 889.4, 889.9 (1:1 ratio); found, 889.3, 889.8 (0.8:1  
657 ratio).

658

659 *Vesicle experiments*

660 *Vesicle preparation procedures:* A mixture of lipids in chloroform solution was evaporated in a  
661 pear shaped flask and held at high vacuum overnight. The resulting lipid film was hydrated with  
662 buffer solution by vortex mixing until all of the lipid material was suspended. The mixture was  
663 subjected to three cycles of freeze- thaw (liquid nitrogen; warm water) to produce a mixture of  
664 vesicles. In some experiments the mixture was additionally sonicated at 3W using a probe  
665 sonicator (three cycles of 20 seconds at 50% duty cycle). The vesicle suspension was then sized  
666 through a 0.1  $\mu\text{m}$  Nucleopore membrane 19 times (Liposofast, Avestin). The sized sample was  
667 filtered on a Sephadex G-25 gel column eluted with the buffer solution used in the preparation.  
668 The first few cloudy drops through the column were discarded and the remaining cloudy fraction  
669 was diluted to a known volume with the buffer. Vesicle diameter was determined by dynamic  
670 light scattering on a Brookhaven Instruments using ZetaPALS particle sizing software. Vesicle  
671 solutions were stored at 5°C and used within 24 hours.

672 *Nitrophenolate release assay*

673 Vesicles were prepared from a mixture of L- $\alpha$ - phosphatidylcholine (50 mg) and **3c** (3.2 wt %),  
674 **7c** (1.5 wt %), or **8c** (1.3 wt %) in a buffer of 0.01 M  $\text{Na}_3\text{PO}_4$ , 0.01 M NaCl with the pH adjusted  
675 to 6.4 using concentrated  $\text{H}_3\text{PO}_4$ ; the initial dispersion was in 0.8 mL of buffer. Final dilution  
676 was to 5.0 mL (~10 mg/mL lipid). Average vesicle diameter: **3c**,  $126 \pm 6$  nm; **7c**,  $148 \pm 11$  nm;  
677 **8c**,  $147 \pm 10$  nm; PDI in all cases ~0.15. In a typical experiment 500  $\mu\text{L}$  of the vesicle solution  
678 was transferred to a 2 mm x 10 mm quartz cell, 10  $\mu\text{L}$  of 1 M NaOH solution was added to the  
679 cell resulting in a solution with pH~11.8. The cell was then transferred to a UV-vis spectrometer  
680 and absorbance at 400 nm was monitored over time. No experiment produced a significant  
681 absorbance change due to nitrophenolate release.

682

683 *NBD-lipid fluorescence quenching assay*

684 Vesicles were prepared from a mixture of lipids (15 mg) consisting of: 70 wt% L- $\alpha$ -  
685 phosphatidyl choline, 25 wt% cholesterol, 3 wt% DSPE-PEG (1,2-distearoyl-sn-glycero-3-  
686 phosphoethanolamine-N-[methoxy(polyethylene glycol)-2000] (ammonium salt)), 2 wt% L- $\alpha$ -  
687 phosphatidic acid and **3c** (0.1 wt%; 0.08 mol%), **7c** (0.2 wt%; 0.08 mol%), or **8c** (0.2 wt%; 0.08  
688 mol%) in a buffer consisting of 0.01 M KCl, 0.01 M HEPES, adjusted with NaOH to pH=7.2;  
689 the initial dispersion was in 0.5 mL of buffer. Final dilution was to 1.00 mL (~15 mg/mL total  
690 lipids). Average vesicle diameter: **3c**,  $132 \pm 8$  nm (PDI  $0.37 \pm 0.01$ ); **7c**  $193 \pm 2$  nm (PDI  $0.13 \pm$   
691  $0.015$ ); **8c**,  $182 \pm 2$  nm (PDI  $0.14 \pm 0.01$ )

692 In a typical experiment, an aliquot of the vesicle solution (100 $\mu$ L) was added to buffer (2.0 mL)  
693 in a 1 cm  $\times$  1 cm quartz cuvette. The sample was magnetically stirred and temperature  
694 equilibrated (25.1 $^{\circ}$ C) for 2 minutes in the fluorimeter. Trial experiments established that 10  $\mu$ L  
695 of CoSO<sub>4</sub> solution (70.7 mM, final diluted concentration 0.2 mM) was sufficient to give  
696 sufficient signal quenching. After temperature equilibration, the aliquot of CoSO<sub>4</sub> solution was  
697 added and the spectrum recorded between 500 and 600 nm ( $\lambda_{\text{ex}}$  470 nm). Vesicles were lysed  
698 with triton solution (5 w/v%, pH=7.2, 25  $\mu$ L) and the spectrum was again recorded. As  
699 described in the text, the reverse order of addition – triton solution before CoSO<sub>4</sub> solution – was  
700 also required to generate a complete series for analysis. The proportion of headgroups in the  
701 outer leaflet is then given as:  $(I_0/I - 1)_{\text{no triton}} / (I_0/I - 1)_{\text{with triton}}$ .

702

703 **Supplementary material**

704 Supplementary material is available with the article through the journal Web site.

705

706 **Acknowledgements**

707 The ongoing support of the Natural Sciences and Engineering Research Council of Canada is  
708 gratefully acknowledged.

709

710

711 **References**

- 712 (1) De Rosa, M.; Gambacorta, A. *Progress in Lipid Research* **1988**, *27*, 153.  
713 (2) Sprott, G. D. In *eLS*; John Wiley & Sons, Ltd: Chichester, 2011, p 12.  
714 (3) Woese, C. *Proceedings of the National Academy of Sciences* **1998**, *95*, 6854.  
715 (4) Fuhrhop, J.-H.; Wang, T. *Chemical Reviews* **2004**, *104*, 2901.  
716 (5) Beveridge, T. J.; Choquet, C. G.; Patel, G. B.; Sprott, G. D. *Journal of Bacteriology* **1993**, *175*,  
717 1191.  
718 (6) Jacquemet, A.; Barbeau, J.; Lemiègre, L.; Benvegna, T. *Biochimie* **2009**, *91*, 711.  
719 (7) Chong, P. L.-G. *Chemistry and Physics of Lipids* **2010**, *163*, 253.  
720 (8) Patel, G. B.; Sprott, G. D. *Crit. Rev. Biotech.* **1999**, *19*, 37.  
721 (9) Brown, D. A.; Venegas, B.; Cooke, P. H.; English, V.; Chong, P. L.-G. *Chemistry and Physics of*  
722 *Lipids* **2009**, *159*, 95.  
723 (10) Tolson, D. L.; Latta, R. K.; Patel, G. B.; Sprott, G. D. *Journal of Liposome Research* **1996**, *6*, 755.  
724 (11) Sprott, G. D.; Dicaire, C. J.; Côté, J.-P.; Whitfield, D. M. *Glycobiology* **2008**, *18*, 559.  
725 (12) Sprott, G. D.; Yeung, A.; Dicaire, C. J.; Yu, S. H.; Whitfield, D. M. *Archaea* **2012**, *2012*, 9.  
726 (13) Eguchi, T.; Ibaragi, K.; Kakinuma, K. *The Journal of Organic Chemistry* **1998**, *63*, 2689.  
727 (14) Delfino, J. M.; Stankovic, C. J.; Schreiber, S. L.; Richards, F. M. *Tetrahedron Letters* **1987**, *28*,  
728 2323.  
729 (15) Markowski, T.; Drescher, S.; Meister, A.; Blume, A.; Dobner, B. *Organic & Biomolecular*  
730 *Chemistry* **2014**, *12*, 3649.  
731 (16) Fuhrhop, J. H.; Fritsch, D. *Accounts Chem. Res.* **1986**, *19*, 130.  
732 (17) Markowski, T.; Drescher, S.; Förster, G.; Lechner, B.-D.; Meister, A.; Blume, A.; Dobner, B.  
733 *Langmuir* **2015**, *31*, 10683.  
734 (18) Fyles, T. M.; Zeng, B. *J. Org. Chem.* **1998**, *63*, 8337.  
735 (19) Moszynski, J.; Fyles, T. M. *J. Am. Chem. Soc.* **2012**, *134*, 15937–15945.  
736 (20) Fyles, T. M. *Accounts Chem. Res.* **2013**, *46*, 2847.  
737 (21) Sakai, N.; Mareda, J.; Matile, S. *Acc. Chem. Res.* **2008**, *41*, 1354.  
738 (22) Maccioni, E.; Mariani, P.; Rustichelli, F.; Delacroix, H.; Troitsky, V.; Riccio, A.; Gambacorta, A.; De  
739 Rosa, M. *Thin Solid Films* **1995**, *265*, 74.  
740 (23) Mathai, J. C.; Sprott, G. D.; Zeidel, M. L. *Journal of Biological Chemistry* **2001**, *276*, 27266.  
741 (24) Jacquemet, A.; Vié, V.; Lemiègre, L.; Barbeau, J.; Benvegna, T. *Chemistry and Physics of Lipids*  
742 **2010**, *163*, 794.  
743 (25) Drescher, S.; Lechner, B.-D.; Garamus, V. M.; Almásy, L.; Meister, A.; Blume, A. *Langmuir* **2014**,  
744 *30*, 9273.  
745 (26) Allen, T. M.; Cullis, P. R. *Adv. Drug Del. Rev.* **2013**, *65*, 36.  
746 (27) Wicki, A.; Witzigmann, D.; Balasubramanian, V.; Huwyler, J. *J. Cont. Rel.* **2015**, *200*, 138.

- 747 (28) Genge, K.; Moszynski, J. M.; Thompson, M.; Fyles, T. M. *Supramol. Chem.* **2012**, *24*, 29.  
748 (29) Moszynski, J. M.; Fyles, T. M. *Org. Biomol. Chem.* **2010**, *8*, 5139.  
749 (30) Luong, H.; Fyles, T. M. *Org. Biomol. Chem.* **2009**, *7*, 733.  
750 (31) Luong, H.; Fyles, T. M. *Org. Biomol. Chem.* **2009**, *7*, 725.  
751 (32) Eggers, P. K.; Fyles, T. M.; Mitchell, K. D. D.; Sutherland, T. J. *Org. Chem.* **2003**, *68*, 1050.  
752 (33) Chui, J. K. W.; Fyles, T. M.; Luong, H. *Beilstein J. Org. Chem.* **2011**, *7*, 1562.  
753 (34) Fyles, T. M.; Hu, C.; Luong, H. *J. Org. Chem.* **2006**, *71*, 8545.  
754 (35) Liang, L.; Astruc, D. *Coordination Chemistry Reviews* **2011**, *255*, 2933.  
755 (36) O'Neil, E. J.; DiVittorio, K. M.; Smith, B. D. *Organic letters* **2007**, *9*, 199.  
756 (37) Forbes, C. C.; DiVittorio, K. M.; Smith, B. D. *Journal of the American Chemical Society* **2006**, *128*, 9211.  
757  
758 (38) Chui, J. K. W.; Fyles, T. M. *Organic & Biomolecular Chemistry* **2014**, *12*, 3622.  
759 (39) Pasini, D. *Molecules* **2013**, *18*.  
760 (40) Chouhan, G.; James, K. *Organic Letters* **2011**, *13*, 2754.  
761 (41) Schulz, M.; Tanner, S.; Barqawi, H.; Binder, W. H. *Journal of Polymer Science Part A: Polymer Chemistry* **2010**, *48*, 671.  
762  
763 (42) Kuang, G.-C.; Guha, P. M.; Brotherton, W. S.; Simmons, J. T.; Stanke, L. A.; Nguyen, B. T.; Clark, R. J.; Zhu, L. *Journal of the American Chemical Society* **2011**, *133*, 13984.  
764  
765 (43) Liu, X.-M.; Thakur, A.; Wang, D. *Biomacromolecules* **2007**, *8*, 2653.  
766 (44) Moss, R. A.; Swarup, S. *Journal of the American Chemical Society* **1986**, *108*, 5341.  
767 (45) Moss, R. A.; Li, J. M. *Journal of the American Chemical Society* **1992**, *114*, 9227.  
768 (46) Moss, R. A.; Okumura, Y. *Journal of the American Chemical Society* **1992**, *114*, 1750.  
769 (47) Chattopadhyay, A. *Chemistry and Physics of Lipids* **1990**, *53*, 1.  
770 (48) Balch, C.; Morris, R.; Brooks, E.; Sleight, R. G. *Chemistry and Physics of Lipids* **1994**, *70*, 205.  
771 (49) Boon, J. M.; Smith, B. D. *Medicinal Research Reviews* **2002**, *22*, 251.  
772 (50) Angeletti, C.; Nichols, J. W. *Biochemistry* **1998**, *37*, 15114.  
773 (51) Morris, S. J.; Bradley, D.; Blumenthal, R. *Biochimica et Biophysica Acta (BBA) - Biomembranes* **1985**, *818*, 365.  
774  
775 (52) *Principles of Fluorescence Spectroscopy*; 3rd ed.; Lakowicz, J. R., Ed.; Springer: New York, USA, 2006.  
776  
777 (53) Heimberg, T. *Thermal Biophysics of Membranes*; Wiley-VCH: Weinheim, 2007.  
778 (54) Israelachvili, J. N.; Marčelja, S.; Horn, R. G. *Quarterly Reviews of Biophysics* **1980**, *13*, 121.  
779  
780